Modal Dispersion Performance of Mode Vector Modulation

F. Barbosa[1,*], F. Ferreira[1], A. Brisson[2], A. Biswas[2], M. Dadras[2], E. Fink[2,4], I. Roudas[2], and X. Jiang[3]

[1]*Dept. of Electronic & Electrical Engineering, University College London, London, WC1E 7JE*
[2]*Dept. of Electrical & Computer Engineering, Montana State University, Bozeman, MT 59717*
[3] *Dept. of Engineering and Environmental Science, CUNY, Staten Island, NY 10314*
[4] *Dept. of Mathematical Sciences, Montana State University, Bozeman, MT 59717*
E-mail: fabio.barbosa@ucl.ac.uk

ABSTRACT Mode vector modulation (MVM) is a new spatial modulation scheme suitable for few-mode/multicore fibers or for multimode transmission in optical wireless links. When used in conjunction with direct-detection in short-haul optical links, MVM offers significantly higher sensitivity compared to M-ary pulse amplitude modulation (M-PAM).

Since MVM uses several spatial and polarization modes simultaneously for transmission of a single data stream, modal effects in few-mode fibers, such as mode coupling and modal dispersion, are potentially of paramount importance and their impact on MVM system performance should be thoroughly understood.

In this invited paper, we study by simulation, for the first time, the transmission of MVM through a few-mode fiber (FMF) with six spatial and polarization modes. We show that, by employing a suitable combination of optical and electronic equalization techniques, the impact of mode coupling and modal dispersion on MVM performance can be significantly reduced. Consequently, it is theoretically possible to replace multiple M-PAM tributaries transmitted in parallel over a fiber bundle with one MVM channel launched over a single FMF in order to decrease the photon and the fiber count in future ultra-high-data-rate, direct-detection optical interconnects.
Keywords: Optical communications, modal dispersion, direct detection, modulation formats.

1. INTRODUCTION

Currently, the most cost-effective multiplexing technology for short-haul optical interconnects is to use multiple parallel fiber lanes and transmit a single wavelength channel per fiber lane. This is a rudimentary form of space-division multiplexing (SDM). In future data centers, the fiber count per link can be reduced by using few-mode and multicore fibers instead of fiber bundles. Assuming weak intermodal/intercore coupling, different modes/cores can be used as separate lightpaths [1]. Alternatively, it is possible to design optical communication systems that use all spatial and polarization modes in few-mode and multicore fibers in unison rather than individually [2], [3]. Such optical communications systems enable the adoption of innovative spatial modulation formats that can be used in conjunction with either coherent or direct detection.

It is worth noting that Stokes vector modulation (SVM) is a spatial modulation format for single-mode fibers (SMFs) [4]. SVM jointly utilizes the x and y states of polarization (SOPs) within SMFs for information transmission. The driving force behind SVM adoption is its superior performance compared to quaternary pulse amplitude modulation (4-PAM), which is currently the modulation format of choice for optical interconnects. On the downside, SVM employs a much more complex direct-detection polarimetric receiver with multiple photodiodes compared to the conventional, single-branch, single-photodiode direct-detection receiver used in 4-PAM. The SVM receiver also includes a multiple-input multiple-output (MIMO) digital signal processing (DSP) to mitigate and compensate polarization rotations in SMFs, enabling retrieval of polarization information transmitted over SMFs at GBd rates [4].

Our research group recently extended the SVM concept to few-mode and multicore fibers or multimode transmission in free space [5], [6], [7], [8], [9], [10], [11], [12]. This novel, multi-dimensional version of SVM is termed mode vector modulation (MVM). MVM utilizes N spatial and polarization degrees of freedom concurrently to transmit an alphabet of M symbols. An illustration of 64 MVM symbols transmitted over a 6-mode FMF is shown in Fig. 1. Since the signal space of MVM has higher dimensionality than those of SVM and PAM, MVM allows for a greater symbol separation using geometric shaping compared to SVM and PAM for the same average power [12]. Consequently, MVM allows for higher energy efficiency compared to both SVM and PAM. This makes MVM a potential candidate for energy-sensitive communications systems, like inter-datacenter optical interconnects (IDC OIs) or free-space optical links [12].

In our previous papers, we focused on the MVM transceiver architecture, the back-to-back performance of optically-preamplified MVM direct-detection receivers, the optimized geometric shaping of the MVM constellation, and the related bit-to-symbol mapping [5], [6], [7], [8], [9], [10], [11], [12]. However, a detailed investigation into the potential susceptibility of MVM to the combined effects of modal crosstalk (XT) and modal dispersion (MD) is lacking. Here, for the first time and through numerical simulations, we explore the impact of these modal effects in few-mode-fiber (FMF)-based short-haul links on the performance of MVM.

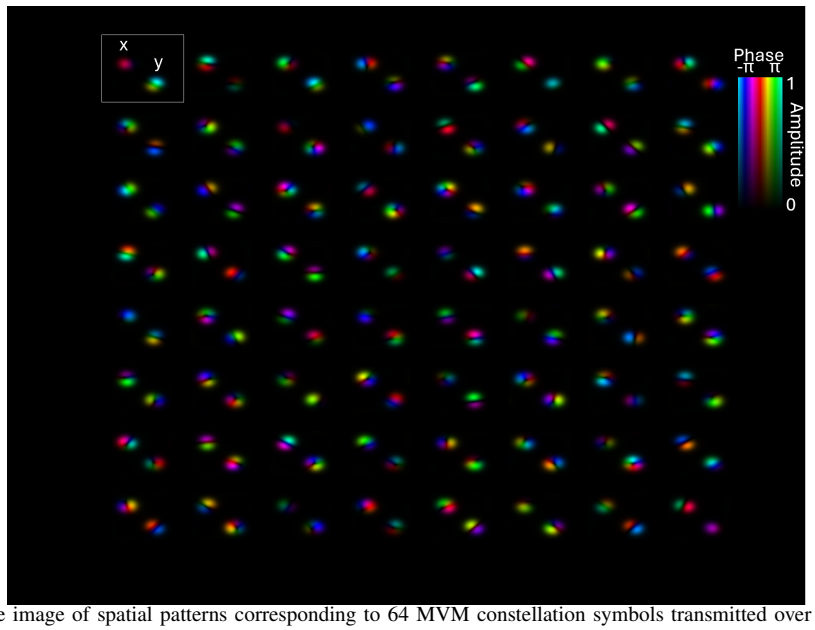

Figure 1: Composite image of spatial patterns corresponding to 64 MVM constellation symbols transmitted over a 6-mode FMF. Intensity and color variations represent different values of amplitude and relative phases, respectively. To avoid clutter, the x and y SOPs are shown separately in a diagonal arrangement. Different variants of MVM are designated by a pair of indices (N, M), where N signifies the total number of spatial and polarization degrees of freedom and M denotes the constellation cardinality. This illustration represents (6,64)-MVM.

We show that using joint optical and electronic MIMO equalization, MVM outperforms both SVM and PAM in terms of energy efficiency.

2. Fiber Model

In the following simulations, we use the multi-section fiber model presented in [13]. In this paper, mode propagation in a given FMF is described by the following set of linear coupled-mode equations, expressed here in the matrix form:

$$\partial_z \tilde{\mathbf{A}}(z,\omega) = -\mathrm{j}[\boldsymbol{\beta}(z,\omega) + \mathbf{K}(z) + \mathbf{R}(z)]\tilde{\mathbf{A}}(z,\omega), \tag{1}$$

where $\tilde{\mathbf{A}}(z,\omega)$ is a column matrix, whose m-th element denotes the spectrum of the slowly-varying electric field complex envelope in mode m; $\boldsymbol{\beta}(z,\omega)$ is a diagonal matrix whose m-th element is the frequency-dependent propagation constant β_m of mode m at a frequency ω; $\mathbf{K}(z)$ is the mode coupling matrix, whose (m,n)-th element is given by the area integral of the inner product of the electric fields of modes m and n, $\mathbf{K}_{mn}(z) = (\omega_0\varepsilon_0/4)\iint \Delta\varepsilon(x,y,z)\boldsymbol{E}_m^*(x,y)\cdot\boldsymbol{E}_n(x,y)\,dx\,dy$, where $\Delta\varepsilon(x,y,z)$ is the relative permittivity perturbation, ω_0 is the carrier angular frequency, and ϵ_0 is the vacuum permittivity; and $\mathbf{R}(z)$ is a block diagonal matrix composed of 2×2 unitary matrices introducing polarization coupling.

In [13], an approximate solution of (1) is obtained by assuming that modal dispersion and linear mode coupling act independently over a sufficiently small fiber length Δz. For a short fiber segment of length Δz, by neglecting dispersive effects and assuming $\boldsymbol{\beta}$, $\mathbf{K}$, and $\mathbf{R}$ are constant over Δz, the fiber transfer matrix is given by

$$\tilde{\mathbf{M}}(\omega) \cong \exp\{-\mathrm{j}\,[\boldsymbol{\beta} + \mathbf{K} + \mathbf{R}]\,\Delta z\}. \tag{2}$$

The propagation constant matrix $\boldsymbol{\beta}$ can be expanded in Taylor series as $\boldsymbol{\beta} = \sum_l \boldsymbol{\beta}_l(\omega-\omega_0)^l$ around the carrier angular frequency ω_0, where $\boldsymbol{\beta}_l$ is a diagonal matrix representing the l-th order derivative of the propagation constant matrix with respect to ω. In this paper, the matrix elements $\boldsymbol{\beta}_m$ and $\mathbf{K}_{mn}$ are obtained from the refractive index profiles optimized for low modal group delay, assuming a graded-index fiber with a cladding

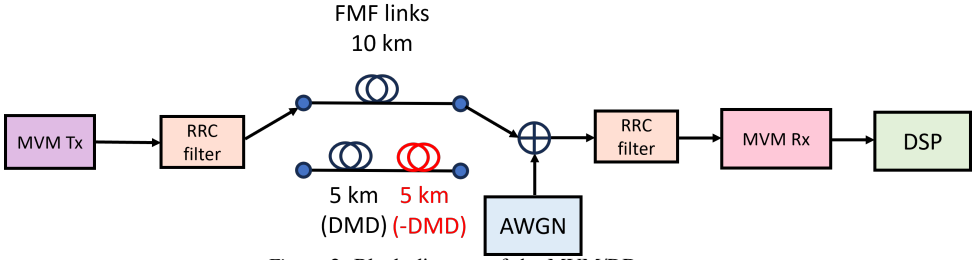

Figure 2: Block diagram of the MVM/DD system.

trench as described in [14]. We also considered the following numerical values for the fiber parameters: a core radius of 6.8 μm, a trench width of 4 μm, a trench depth of -0.0034, a core graded-index exponent of 1.95, and a core-cladding refractive index relative difference of 1%. The coefficients $\boldsymbol{\beta}_m$ are kept constant over all fiber sections, while the elements $\mathbf{K}_{mn}$ change given a random radial and azimuthal offset in each section. Finally, the end-to-end fiber transfer matrix $\mathbf{H}(\omega)$ is the product of the transfer matrices of different sections in the form given by (2), i.e., $\mathbf{H}(\omega) = \tilde{\mathbf{M}}_K(\omega) \cdot \tilde{\mathbf{M}}_{K-1}(\omega) \cdot \tilde{\mathbf{M}}_{K-2}(\omega) \ldots \cdot \tilde{\mathbf{M}}_1(\omega)$, where K represents the total number of fiber sections.

3. SIMULATION SETUP

The block diagram of an MVM/DD point-to-point optical transmission system is depicted in Fig. 2. At the transmitter, ideal MVM signals of various dimensionalities N and constellation cardinalities M can be generated. These signals correspond to geometrically-optimized constellations and bit-to-symbol mappings following the procedures described in [12]. MVM pulses are shaped using a root-raised cosine (RRC) filter and then launched into a FMF.

In the simulation block diagram of Fig. 2, we consider two possible fiber configurations: In the first case, we use a single FMF type for the entire span (MD-unmanaged link). In the second case, we use two different FMF types in series to reduce modal dispersion, a transmission fiber for the first half and a compensating fiber for the second half of the span, respectively (MD-managed link). The rationale behind the second approach is that, for weak intermodal coupling, the DMD can be greatly reduced by cascading two FMFs of equal length with opposite modal dispersion characteristics. Notably, an FMF can be engineered with opposite uncoupled DMDs by controlling the core grading exponent [15].

Pulse propagation is performed using the fiber model described in the previous section based on matrix concatenation to represent short fiber segments corresponding to a distorted core-cladding boundary. The simulation model encompasses all major linear impairments, including attenuation due to Rayleigh scattering and macrobend loss (MBL), differential mode delay (DMD), and linear mode coupling. These impairments are calculated for a trench-assisted, graded-index fiber optimized according to [14]. Monte Carlo simulations are tailored for a desired average intermodal crosstalk (XT) per unit length, typical for FMFs [13]. To achieve the target average intermodal XT per unit length, the core-cladding radial displacement of fiber sections is adjusted accordingly. To broaden the analysis, the actual (uncoupled) DMD of the designed FMF is artificially scaled to match a desired value. Alternatively, a similar outcome could be attained by redesigning the fiber to possess a specific DMD using the procedure outlined in [14].

All simulations are conducted in the absence of chromatic dispersion (CD), assuming that the latter can be compensated by operating in the O-band [16].

Amplified spontaneous emission (ASE) noise is modeled by noise loading at the receiver using an additive white Gaussian noise (AWGN) source. Following noise loading, signals undergo filtering using an optical matched RRC filter [12]. An ideal, noiseless, mode-vector direct-detection polarimetric receiver is assumed. The receiver is modeled as a black box that performs a transformation of the received symbols from the generalized Jones space to the generalized Stokes space [12].

Subsequently, the digital signal processing (DSP) unit [12] counteracts the polarization rotations that occur during fiber propagation. It operates in Stokes space and multiplies the received Stokes vectors with of a Müller matrix, whose elements are adjusted in a recursive fashion using the least-mean square (LMS) algorithm [12]. The LMS algorithm uses a data-aided approach for an initial batch of received samples before transitioning to a decision-directed approach for the remaining samples. After derotating the received symbols, maximum-likelihood estimation is conducted in Stokes space [12], and the bit error rate (BER) is computed.

In this paper, we consider a 10-km 6-mode fiber that supports the LP_{01} and LP_{11} mode groups. Since each spatial mode consists of two orthogonal SOPs, the number of spatial and polarization degrees of freedom is $N = 6$. We divide the fiber into equal sections of 1-100 m length each depending on the value of intermodal crosstalk per unit length. Unless otherwise stated, a target average intermodal crosstalk per unit length of -30 dB/km is assumed. The FMF is initially designed for an MD parameter of 0.1 ps/km. The transmitter and receiver RRC filters have a roll-off factor of 1. The LMS algorithm uses a data-aided approach for the initial 3,000 received symbols before transitioning to a decision-directed approach for the remaining symbols. The step size is fixed at 0.001 for all cases.

For a fair comparison, all modulation formats considered here have the same spectral efficiency per spatial degree of freedom. More specifically, in the next section, we compare the performance of (6,64)-MVM over a 6-mode FMF against that of three 4-PAM or 4-SVM tributaries transmitted over three SMF lanes. In all cases, we transmit an average of 2 bits per symbol per spatial degree of freedom. Standard IDC OI symbol rates R_s of 56 and 112 GBd are considered, accounting for 12% Ethernet and KP4 FEC overhead.

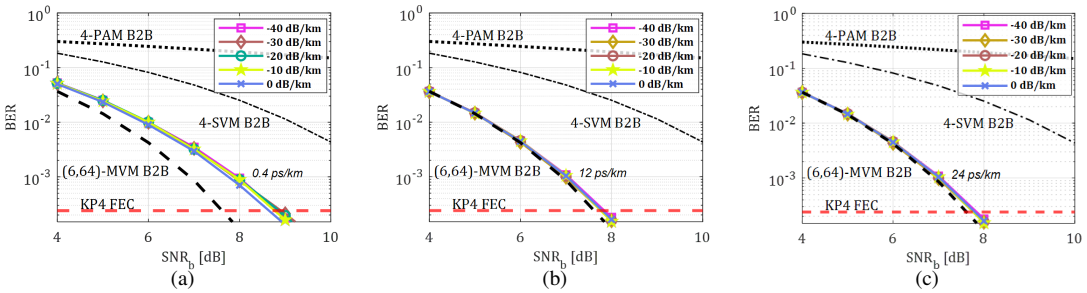

Figure 3: $(6, 64)$-MVM performance for MD-managed and MD-unmanaged links with various levels of modal coupling [dB/km]. All figures assume a total link length of 10 km, R_s = 56 GBd, and 0 ps intramodal delay between the LP_{11} modes. Back-to-back (B2B) performance curves for 4-PAM, 4-SVM, and (6,64)-MVM are included for comparison. (a) MD-unmanaged link with MD-parameter = 0.4 ps/km; (b) MD-managed link with MD-parameter = 12 ps/km; (c) MD-managed link with MD-parameter = 24 ps/km.

4. Results and Discussion

In the simultaneous presence of mode coupling and modal dispersion, we anticipate that the relative positions of the Stokes vectors of the MVM constellation will change, i.e., the constellation shape will become suboptimal, and the performance of the mode-vector direct-detection receiver will deteriorate. If the SNR penalty at the KP4 FEC threshold is significant (on the order of several dB), the back-to-back superiority advantage of MVM in terms of receiver sensitivity over standard modulation formats [12] will be diminished or lost.

BER curves for (6,64)-MVM as a function of the bit signal-to-noise ratio SNR_b are depicted in Fig. 3 (solid lines). Each data point on these curves represents an average over 10 different channel realizations with an average crosstalk per unit length of -30 dB/km. For comparison, back-to-back (B2B) results for (6,64)-MVM, 4-PAM, and 4-SVM are also provided (dashed, dotted, and dot-dashed curves, respectively). For single-mode fibers (SMFs), in the absence of chromatic dispersion (CD), the impact of polarization mode dispersion (PMD) on the latter two modulation formats is negligible, resulting in transmission performance equal to the B2B case.

Figure 3a shows results for the MD-unmanaged link at 56 GBd. We observe that after transmission over the 6-mode FMF, (6,64)-MVM experiences only a slight penalty compared to the B2B case when the MD parameter is 0.1 ps/km. However, increasing the MD parameter beyond 0.4 ps/km significantly affects system performance. For MD parameters exceeding 1 ps/km, the sensitivity advantage of (6,64)-MVM over 4-SVM is lost.

Figure 3b and Figure 3c present results for a MD-managed link for symbol rates of 56 and 112 GBd, respectively. Optical compensation of MD helps mitigate the impact of group delay spread on BER. In this case, we observe that MD parameters up to 1 ps/km have minimal impact on system performance for both symbol rates. Moreover, the sensitivity of (6,64)-MVM surpasses that of 4-SVM and 4-PAM for MD parameters up to 48 and 24 ps/km for 56 and 112 GBd, respectively.

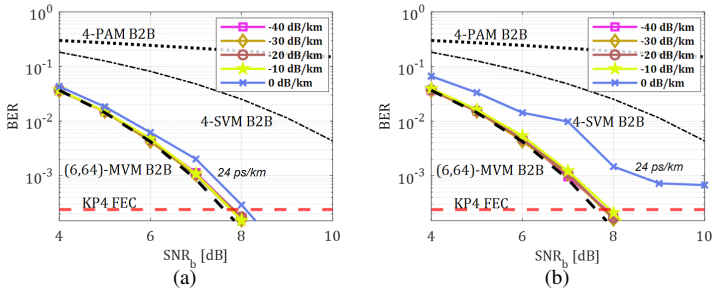

Figure 4: $(6, 64)$-MVM performance for MD-managed links with various levels of modal coupling [dB/km] and intramodal delay between the LP_{11} modes. All figures assume a total link length of 10 km and MD-parameter = 24 ps/km. (a) R_s = 56 GBd and intramodal delay = 1 ps; (b) R_s = 112 GBd and intramodal delay = 1 ps.

Next, we study the impact of intermodal coupling on the curves of Fig. 3 that exhibit an SNR penalty within 2 dB from the B2B case. Fig. 4a illustrates the case of an MD-unmanaged link with an MD parameter of 0.4 ps/km. We observe that the level of intermodal coupling has negligible impact on the performance of (6,64)-MVM. Similarly, for the MD-managed link, we study the impact of intermodal coupling on the curves corresponding to MD parameters 24 ps/km and 12 ps/km for the symbol rates of 56 GBd and 112 GBd, respectively (see Figs. 4b and **??**). For XT levels in the range -60 dB/km to 0 dB/km, we observe once again a negligible impact on MVM system performance.

For mode-division multiplexed systems, strong intermodal coupling is potentially beneficial. However, somewhat surprisingly, strong intermodal coupling appears to have a negligible impact on the performance of spatial

modulations. We observe that modal dispersion is equally detrimental in the presence of both weak and strong mode coupling.

From the above results, we can draw the following conclusions: In the presence of weak intermodal coupling, the 6×6 fiber transfer matrix is approximately a block matrix composed of 2×2 and 4×4 submatrices. At the same time, there is always strong coupling between polarization components within the LP_{01} mode and strong intramodal and cross-polarization coupling within the LP_{11} mode group. For the choice of the modulation format, we must take into account the fact that the joint action of the modal dispersion and mode coupling cannot be undone in mode vector direct-detection receivers. Therefore, in the presence of weak intermodal coupling, the block diagonal structure of the 6×6 fiber transfer matrix guides us into using LP_{01} and LP_{01} as separate lightpaths, i.e., launching SVM constellations ($N = 2$) over the LP_{01} mode group and launching separate MVM constellations with $N = 4$ over the LP_{11} mode group. In theory, using a larger number of modes in unison is more beneficial in terms of receiver sensitivity [12]. On the downside, this benefit in terms of receiver sensitivity is obtained by increasing hardware complexity, i.e., the number of photodiodes and analog-to-digital converters scales with N at best as $3N - 2$ and at worst as $O(N^2)$ [12]. As a conclusion, it is more practical to use MVM modulations on a per spatial mode basis both in terms of simplified signal processing and receiver complexity, at the expense of receiver sensitivity.

5. SUMMARY

We examined how modal dispersion affects MVM transmission across FMFs in both managed and unmanaged links, considering realistic levels of modal crosstalk. Our simulation results indicate that, when using joint optical and electronic MIMO equalization, MVM outperforms both SVM and PAM in terms of energy efficiency. This energy efficiency advantage translates into a bit rate-distance product above the 1 Tbps·km mark.

ACKNOWLEDGEMENTS

This work was supported by NSF Awards 1911183 and 1910140, AFRL Grant FA8750-20-1-1004, as well as and by UKRI Future Leaders Fellowship MR/T041218/1. Underlying data can be found at doi.org/10.5522/04/24788310.

REFERENCES

[1] P. J. Winzer, R. Ryf, and S. Randel, *Optical Fiber Telecommunications VIB: Chapter 10. Spatial Multiplexing Using Multiple-Input Multiple-Output Signal Processing*. Elsevier, 2013.

[2] T. A. Eriksson, P. Johannisson, B. J. Puttnam, E. Agrell, P. A. Andrekson, and M. Karlsson, "K-over-L multidimensional position modulation," *Journal of Lightwave Technology*, vol. 32, no. 12, pp. 2254–2262, 2014.

[3] B. J. Puttnam, T. A. Eriksson, J.-M. D. Mendinueta, R. S. Luís, Y. Awaji, N. Wada, M. Karlsson, and E. Agrell, "Modulation formats for multi-core fiber transmission," *Opt. Express*, vol. 22, no. 26, p. 32457, Dec. 2014.

[4] K. Kikuchi and S. Kawakami, "Multi-level signaling in the Stokes space and its application to large-capacity optical communications," *Opt. Express*, vol. 22, no. 7, p. 7374, 3 2014.

[5] I. Roudas, J. Kwapisz, and E. Fink, "Mode vector modulation," in *European Conference on Optical Communication (ECOC)*, 9 2021, paper Tu2D.5.

[6] E. Fink, J. Kwapisz, and I. Roudas, "Optimized SVM constellations for SDM fibers," in *2021 IEEE Photonics Conference (IPC)*, 2021, paper TuE3.2.

[7] J. Kwapisz, I. Roudas, and E. Fink, "Error probability of mode vector modulation optically-preamplified direct-detection receivers," in *Conference on Lasers and Electro-Optics (CLEO)*, 2022, paper SM4J.1.

[8] J. Kwapisz, I. Roudas, E. Fink, and A. Biswas, "Mode vector modulation direct-detection receivers with linear hardware complexity," in *2022 IEEE Photonics Conference (IPC)*, 2022, paper TuF1.3.

[9] J. Kwapisz, I. Roudas, and E. Fink, "Polarimetric direct detection for spatial superchannels," in *2022 Asia Communications and Photonics Conference (ACP)*, Shenzhen, China, 2022, pp. 670–673.

[10] I. Roudas, E. Fink, and J. Kwapisz, "Mode vector modulation: Optimal signal sets with geometric shaping," in *2023 Optical Fiber Communications Conference and Exhibition (OFC)*, 2023, paper Th3E.4.

[11] I. Roudas, J. Kwapisz, and E. Fink, "Mode vector modulation: A review," in *2023 23rd International Conference on Transparent Optical Networks (ICTON)*, Bucharest, Romania, June 2023, paper We.D2.3.

[12] J. Kwapisz, I. Roudas, and E. Fink, "Mode vector modulation: Extending Stokes vector modulation to higher dimensions," *Journal of Lightwave Technology*, vol. 42, no. 6, pp. 1966–1990, 2024.

[13] F. M. Ferreira, C. S. Costa, S. Sygletos, and A. D. Ellis, "Semi-analytical modelling of linear mode coupling in few-mode fibers," *Journal of Lightwave Technology*, vol. 35, no. 18, pp. 4011–4022, 2017.

[14] F. M. Ferreira and F. A. Barbosa, "Maximizing the capacity of graded-index multimode fibers in the linear regime," *Journal of Lightwave Technology*, vol. 42, no. 5, pp. 1626–1633, 2024.

[15] R. Rath, D. Clausen, S. Ohlendorf, S. Pachnicke, and W. Rosenkranz, "Tomlinson–Harashima precoding for dispersion uncompensated PAM-4 transmission with direct-detection," *Journal of Lightwave Technology*, vol. 35, no. 18, pp. 3909–3917, 2017.

[16] F. Ferreira, D. Fonseca, and H. Silva, "Design of few-mode fibers with arbitrary and flattened differential mode delay," *IEEE Photonics Technology Letters*, vol. 25, no. 5, pp. 438–441, 2013.